

Werk

Jahr: 1984

Kollektion: fid.geo

Signatur: 8 Z NAT 2148:55

Digitalisiert: Niedersächsische Staats- und Universitätsbibliothek Göttingen

Werk Id: PPN1015067948_0055

PURL: http://resolver.sub.uni-goettingen.de/purl?PPN1015067948_0055

LOG Id: LOG_0038

LOG Titel: A new pulsed audiomagnetotelluric technique

LOG Typ: article

Übergeordnetes Werk

Werk Id: PPN1015067948

PURL: <http://resolver.sub.uni-goettingen.de/purl?PPN1015067948>

OPAC: <http://opac.sub.uni-goettingen.de/DB=1/PPN?PPN=1015067948>

Terms and Conditions

The Goettingen State and University Library provides access to digitized documents strictly for noncommercial educational, research and private purposes and makes no warranty with regard to their use for other purposes. Some of our collections are protected by copyright. Publication and/or broadcast in any form (including electronic) requires prior written permission from the Goettingen State- and University Library.

Each copy of any part of this document must contain these Terms and Conditions. With the usage of the library's online system to access or download a digitized document you accept the Terms and Conditions.

Reproductions of material on the web site may not be made for or donated to other repositories, nor may be further reproduced without written permission from the Goettingen State- and University Library.

For reproduction requests and permissions, please contact us. If citing materials, please give proper attribution of the source.

Contact

Niedersächsische Staats- und Universitätsbibliothek Göttingen
Georg-August-Universität Göttingen
Platz der Göttinger Sieben 1
37073 Göttingen
Germany
Email: gdz@sub.uni-goettingen.de

A new pulsed audiomagnetotelluric technique

P.-A. Schnegg and Gaston Fischer

Observatoire Cantonal, CH-2000 Neuchâtel, Switzerland

Abstract. Audiomagnetotellurics (AMT) is a handy tool for probing the electrical structure of the Earth to shallow depths of 1 or 2 km, but is known to be sensitive to man-made perturbations of the source fields. A method with an artificial source in the form of simple current pulses is proposed to overcome these difficulties. The AMT responses to these pulses are stacked additively into a memory. The artificial signal amplitudes thus grow like the number of stacked samples. Noise and uncorrelated natural signals only grow like the root of this number so that the ratios of correlated to uncorrelated amplitudes also grow with the root of the stacking number. This method is broad-band; an ordinary natural AMT station can therefore be used as receiver and it is possible to compare the active and natural source results at once. Because of power limitation the receiver is in the near-field of the source. By placing the source at various distances from the sounding site data are obtained which can be extrapolated to the far-field limit. The logarithm of the apparent resistivity, in particular, is shown to approach the far-field limit as the inverse of the distance. But this approach is polarization-dependent and it is seen that sources in an electrically collinear configuration with the receiving electrodes yield apparent resistivities that are usually much too large. These features explain the frequent large scatter of natural AMT data, as well as apparent resistivities which are often systematically too large by factors of up to an order of magnitude, especially in highly resistive areas.

Key words: Active audiomagnetotellurics – Local perturbations in audiomagnetotellurics

Introduction

Audiomagnetotellurics (AMT) is probably one of the most suitable methods for sounding the electrical properties of the first 1 or 2 km of the Earth's crust. Its implementation, however, even in sparsely populated areas with little industry, is hindered by the important problem of electromagnetic noise which is known to

lead to large dispersions in the measurements. Furthermore, AMT seems to yield apparent resistivities ρ_a which are systematically too large. This arises, we believe, because the signal source, which is assumed to be at very large distances, is in fact often in the vicinity of the structure investigated. The signals recorded are then caused by stray currents generated by such close artificial sources. In addition, these sources are poorly localized and sometimes even moving, as with electric railways.

A demonstration of the poor coherence of the incident or primary signal can be obtained by recording the magnetic field simultaneously at two stations only 1 km apart, over a structure with essentially horizontal stratification, and in an area of low population density. It is seen in Fig. 1 that coherency is already poor at the long periods ($T=0.3-0.1$ s) and becomes much worse toward the shorter ones ($T=0.01-0.001$ s). This has already been invoked (Fischer, 1982) as a likely reason why the "remote magnetic reference method" of Gamble et al. (1979a,b) seems ineffective at AMT frequencies. Evidently these signals appear as if originating from uncorrelated sources. The inducing field cannot be taken as horizontally uniform and the basic premise for AMT sounding is not realized. Our experiments show that if a powerful local source dominates all the others, the apparent resistivity curve is shifted to larger values, sometimes up to a factor of 10 or even more. On the other hand, with a collection of randomly distributed sources of similar power the AMT data also become widely scattered. This effect is particularly marked over highly resistive terrain ($\rho_a > 1000 \Omega\text{m}$; cf., e.g., Schnegg et al., 1984). In the Jura limestone the perturbations propagate over great distances on account of the large penetration depths. Artificial perturbations can therefore render AMT soundings impossible even in remote areas.

The idea of controlling the source is an old one [cf. the recent review by Ward (1984), which contains a fairly exhaustive list of references to such methods], and the main advantages expected from a strong artificial signal with synchronous detection are, naturally, a greater reproducibility and a smaller scatter of AMT sounding data. But such improvements cannot be achieved without paying a price: increased complexity in instrumentation and logistics as well as a smaller

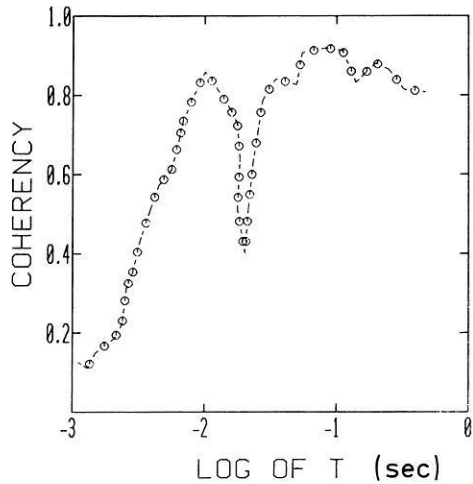


Fig. 1. Coherency vs. period between NS magnetic field variations recorded at two sites 1 km apart. The strong depression at 50 Hz probably occurs because of a rejection filter in our electronics, as well as from the generation of incoherent secondary signals by all mains users

number of soundings per work-day. On the other hand, it may be possible to work with sensing coils and amplifiers of lower sensitivity but possibly with a wider period range: their intrinsic noise may be allowed to reach the level of the external signals, i.e. natural fields plus man-made perturbations, since with such active techniques the natural signals must be regarded as a contribution to all other sources of background noise. The advantage of working with a "standard natural-field AMT system" is that results of the natural and artificial AMT soundings can be compared immediately, without requiring any modification in the deployment of sensing coils or electrodes. The system we have devised embodies this property, which partly explains its rather narrow period range of $T=0.001-0.3$ s.

With the power of a few kilowatts generally available when performing pulsed AMT, it is practically impossible to place the transmitter at distances large enough to guarantee the condition of a uniform incident field (the far-field condition) while providing enough signal at the receiver station. To ensure a sufficient signal level it is necessary to bring the transmitter closer to the receiver, and the ensuing non-uniformity of the field has to be taken care of by an artifice which will be described below. Furthermore, if the complete tensorial information is required at a given site, it is necessary to transmit pulses with at least two different polarizations. There is no equivalent constraint with natural AMT, since the incident fields usually come with a variety of polarizations.

Pulsed AMT technique

The method we have developed can be implemented with little and rather light additional equipment to generate the required signal pulses. At the receiving end a standard microprocessor-controlled AMT station is

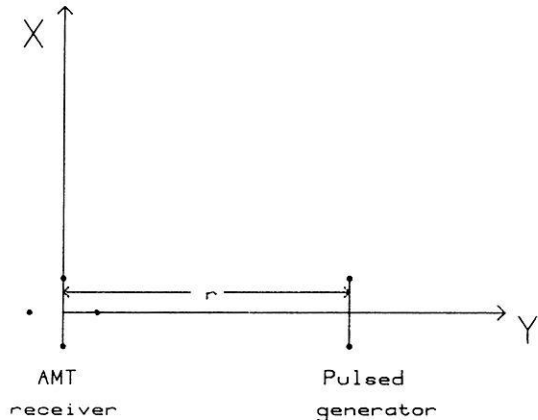


Fig. 2. Layout of receiving and generating stations. Current injection is in a geometry akin to a grounded electric dipole. The configuration represented here is termed "broadside-y". When the injection electrodes are both on the y-axis we call it "collinear-y". Similarly, there are "broadside-x" and "collinear-x" geometries. For distances r up to 500 m the injection electrodes are 25 m apart; for larger distances the spacing is 100 m

used, with only minor software modifications and the sole addition of an accurate quartz clock. As was said above, this has the important advantage that controlled source and natural source soundings can be performed in succession without moving any equipment, except switching the microprocessor to another mode of data management. Deploying the instruments at a given site takes 10 min. Sounding with the pulsed source, including a natural source sounding in the range $T=0.001-0.3$ s, may require 3-4 h.

The transmitter consists of a 220 V ac gasoline generator which delivers 2 kW of power into an autotransformer. With a motor drive the output can be varied with a linear ramp from 0 to 220 V in 4 s. This variable voltage is multiplied by a fixed-ratio transformer, rectified and fed into a condenser bank of 200 μ F total capacity. At the end of the charging cycle the bank voltage reaches 4,300 V. The condensers are discharged periodically into the ground at 5-s intervals. Thanks to the high initial voltage, the discharge can be effected through ordinary metal spikes that are simply driven to a depth of about 20 cm into the ground, with which they ensure a sufficiently good contact that an initial current of 20 A is easily achieved. The spacing of these current electrodes is typically 25 or 100 m and the overall configuration is shown in Fig. 2. With the generator at a distance of 500 m, the field ratios observed have always been identical, whether injection was carried out with an electrode separation of 25 m or 100 m, but the field amplitude increases approximately in proportion to the electrode spacing, and the wider spacing is therefore used when injecting at 500 m or beyond. A regular rate of one pulse every 5 s is ensured through a second quartz clock. Other pulse rates can, of course, be chosen.

The five AMT signals sampled (two telluric and three magnetic channels) are stacked into the RAM memory of a microcomputer which controls the entire

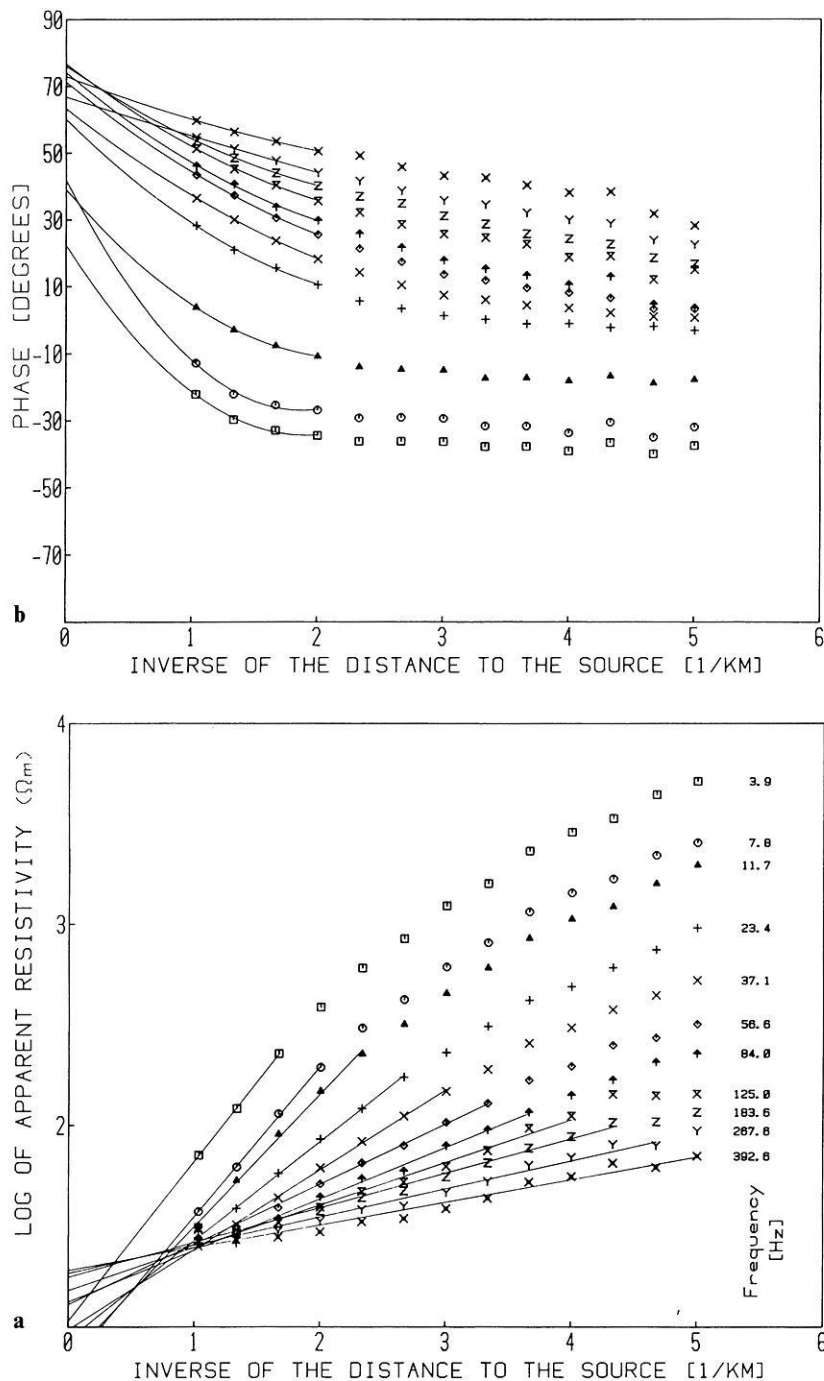


Fig. 3a and b. **a** Plot of the logarithm of apparent resistivity vs the inverse of distance for a broadside geometry at an approximately one-dimensional site. Note the linear approach to the $1/r \rightarrow 0$ limit and the systematically increasing resistivities when the source is moved closer. **b** Phase lag ψ between electric and magnetic fields for the same sounding. The phase appears to assume a linear behaviour with $1/r$ at much larger distances only; extrapolation was therefore effected quadratically, as explained in the Appendix, taking into account the four most distant sites. Note that the phase lag seems to be systematically less for sources at closer range, with the electric field even sometimes ahead of the magnetic field

data management of the receiving station (Fischer, 1982). The two quartz clocks are monitored by timing pulses from a regular transmitter of time signals (HBG, but DCF, MSF, OMA, JG2, or WWVB, e.g., can be used in other areas). They control the sequences of pulse firing, signal sampling, analog to digital conversion, and stacking. By this stacking process the amplitude of the artificially generated signals increases in proportion to the number of pulses, whereas the uncorrelated natural signal and the noise only increase as the root of that number. The ratio of correlated to random signals thus also increases as the root of the pulse number. Usually 50–100 samples are stacked; by then the signal ratio is strong enough and can be

processed as if it were a classical AMT signal, yielding apparent resistivity and phase. Because the injected current pulse takes a form resembling an exponential decay, its Fourier spectrum is broadband and contains adequate energy in the period band of $T=0.001-0.3$ s that we process. Contrary to natural AMT, where apparent resistivity $\rho_a(T)$ and phase $\phi(T)$ are averaged over a large number of such samples (typically 50–100), computation in this form of artificial AMT is carried out only once, after the stacking is completed. When the structure is not horizontally layered (one-dimensional=1D), it is necessary to carry out the injection in at least two different directions, usually chosen at a right angle (cf. Fig.2) and, in principle at least, the

entire impedance tensor Z can then be derived. As will be seen later, the collinear geometries are less favourable; it is preferable to determine the impedance tensor from the two broadside geometries.

Preliminary pulsed AMT results

The limited source power available is generally not sufficient to realize the condition of a very distant source, under which the incident signal can be considered equivalent to a plane wave. This is particularly true at our longest periods of 0.3 s. As a consequence, the data are biased by the proximity of the source, as shown in Fig. 3. This figure shows how the apparent resistivity changes as the source is placed at various distances. These data were obtained in a broadside configuration over a good conductor, a dried-up marsh. It is worth looking at the behaviour of $\rho_a(T)$, the apparent resistivity at a given period, as a function of source distance r , or rather of $\log \rho_a$ as a function of the inverse distance $1/r$. This reveals that the asymptotic behaviour of $\log \rho_a$ vs $1/r$ is linear when r becomes very large. For the various periods T the $\log \rho_a$ values line up on a set of straight lines, as shown in Fig. 3a. This behaviour has been confirmed theoretically in the Appendix with expressions for the fields $\mathbf{E}(\mathbf{r})$ and $\mathbf{H}(\mathbf{r})$ derived by Goldstein and Strangway (1975) for a horizontal two-layer structure. Clearly, the values extrapolated to $1/r=0$ are those that correspond to a source at infinity. If one works in the range where $\log \rho_a$ is linear with $1/r$, it is therefore possible to obtain correct $\rho_a(T)$ values by placing the source at three or four different distances, *but in the same direction* with respect to the AMT receiving station.

In general, it will be observed that collinear injection produces a much stronger dependence with distance than broadside injection. This means that the slope of the linear portion of $\log \rho_a$ vs $1/r$ is much

stronger, and the intercept at $1/r=0$ is not as clearly defined. This is quite evident in Fig. 4, where it can also be seen that ρ_a reaches very large values at short range, i.e. when $1/r$ increases. This is an important observation: it demonstrates the strong increase of $\rho_a(T)$ caused by perturbations in a collinear geometry, even at fairly long range. Theoretical and experimental confirmation of this behaviour is given by Goldstein and Strangway (1975), who also show that various other geometries are unsuitable because of particular polarizations of the fields; for example, with broadside- x injection there is no E_x field on the x -axis over an ideal 1 D structure.

It is instructive to compare the natural AMT sounding results at a given site with those extrapolated to a source at infinity, which were obtained with the controlled source. We see in Fig. 5 that the former indeed yields apparent resistivities which are systematically larger by about a factor of two and are more dispersed than the controlled source results, and the deviation increases with the period. If the natural curve of Fig. 5 is placed over the family of controlled source curves of Fig. 6, where the source distance is a parameter, it appears as if the natural data were produced by a source at about 1.5 km. Figures 5 and 6 thus provide a clear demonstration that, in this case at least, the natural source cannot be assumed to be infinitely remote. The short distance found is in fact suggestive of local sources, either extended sources at somewhat greater distances (industry, electric trains, power lines) or closer and more compact sources (small factories, electric farm machinery, households). This observation is obviously an important one; it has generally been overlooked but may explain many poor sounding results and especially the often strikingly higher resistivities derived from AMT than from geoelectric soundings.

Figures 7 and 8 display data obtained under conditions of more severe perturbations and provide a

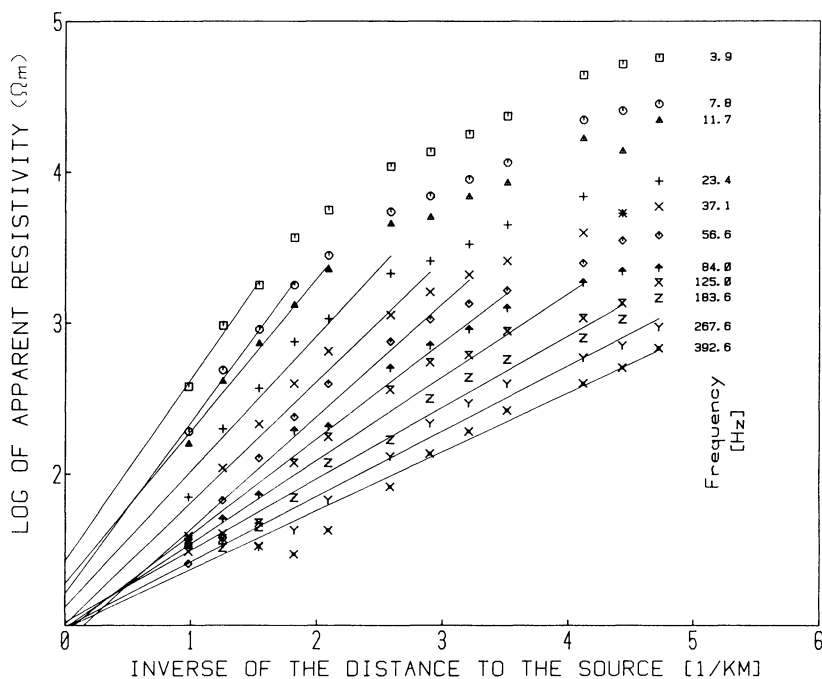


Fig. 4. Sounding results at the same site as for Fig. 3, but with collinear injection. Note the stronger variation with $1/r$ and the much larger apparent resistivities for close sources

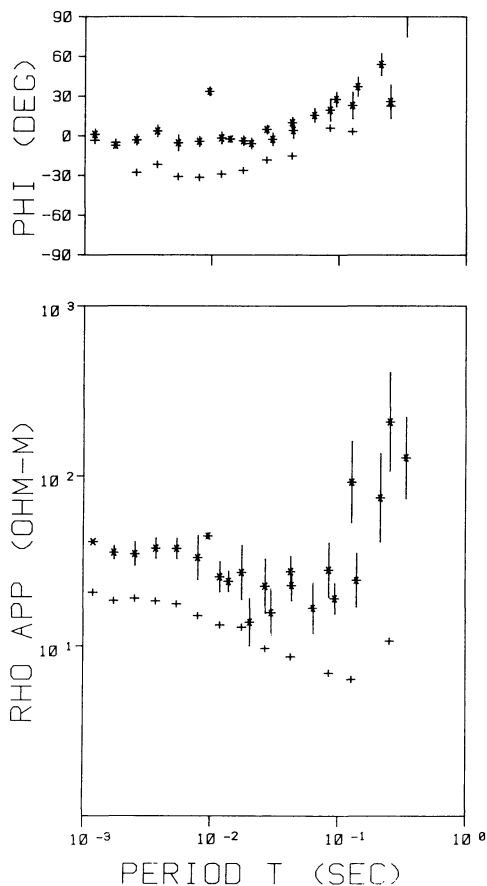


Fig. 5. Pulsed AMT sounding results derived from the Fig. 3a and b data (crosses) and results from natural field AMT (stars with error bars). For the phase we have plotted $\phi = 45^\circ - \psi$, such that ϕ vanishes for a uniform medium and exhibits a positive main excursion for a substratum more resistive than the top layer. Note the systematically larger resistivities and phases ϕ derived from the natural field sounding

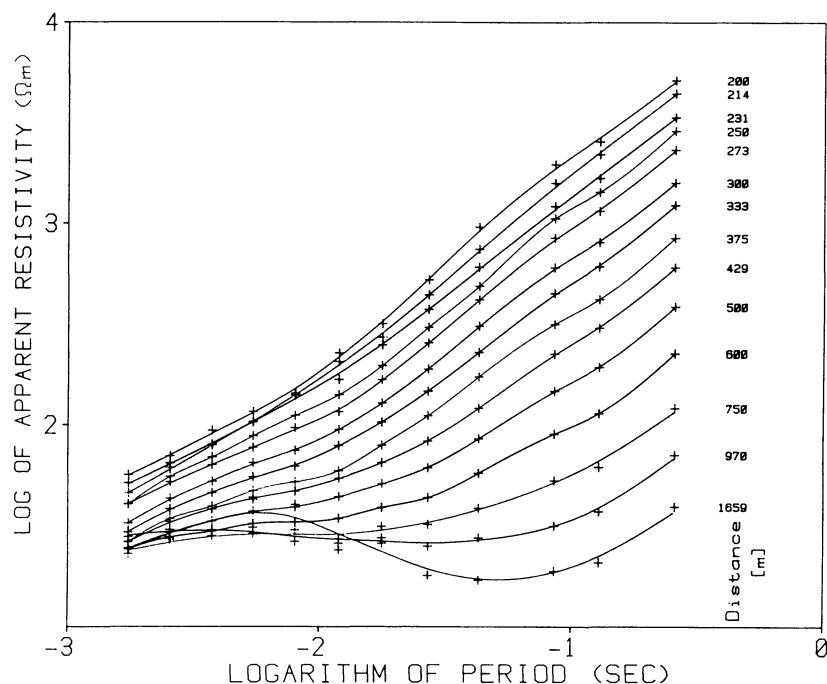


Fig. 6. Logarithm of apparent resistivity vs logarithm of period, with distance r as a parameter, for broadside injection at the same site as for Figs. 3-5. The comparison with Fig. 5 suggests that for this sounding site the natural field data appear as if resulting from a point source at about 1.5 km. With collinear injection the same distortion has already arisen when the source is even further away. The small undulations of the curves may be a consequence of the imperfect one-dimensionality of the structure

strong confirmation of the statements in the previous paragraph. The site is a highly resistive dense limestone with a thin overburden, only 1 or 2 m thick, of good conducting sediments. Again, natural AMT is seen to yield apparent resistivities systematically too large by a factor close to an order of magnitude.

Assessment of the new method

One-dimensional structures

So far we have directed our attention almost exclusively toward 1 D structures, even though the practical results we have shown may not refer to perfect horizontal layering. The method is well suited to the study of such simple structures: for the apparent resistivity ρ_a it is easy to reach the distance range where $\log \rho_a$ varies linearly with the inverse distance $1/r$ (see Appendix); for the phase ψ it is necessary to work with a quadratic extrapolation, but as we have shown for the data of Fig. 3b, this presents no great difficulty. Furthermore, 1 D structures can be modelled even in the absence of phase data (cf. Fischer and Le Quang 1981, 1982; Fischer and Schnegg, 1980).

Another feature which simplifies the experimental study of 1 D structures by the new method is the fact that it suffices to move the source along a single direction, preferably in a broadside configuration. However, in most instances it will be advisable to work with both broadside geometries precisely to obtain proof that the structure is effectively 1 D.

Localized anomalies within 1 D structures

AMT is now frequently used to investigate 2 D or 3 D geological accidents within structures which, at large distances, become simply 1 D. Typical examples are intrusions or faults (Schnegg et al., 1984). The pulsed AMT method will remain useful here, in particular

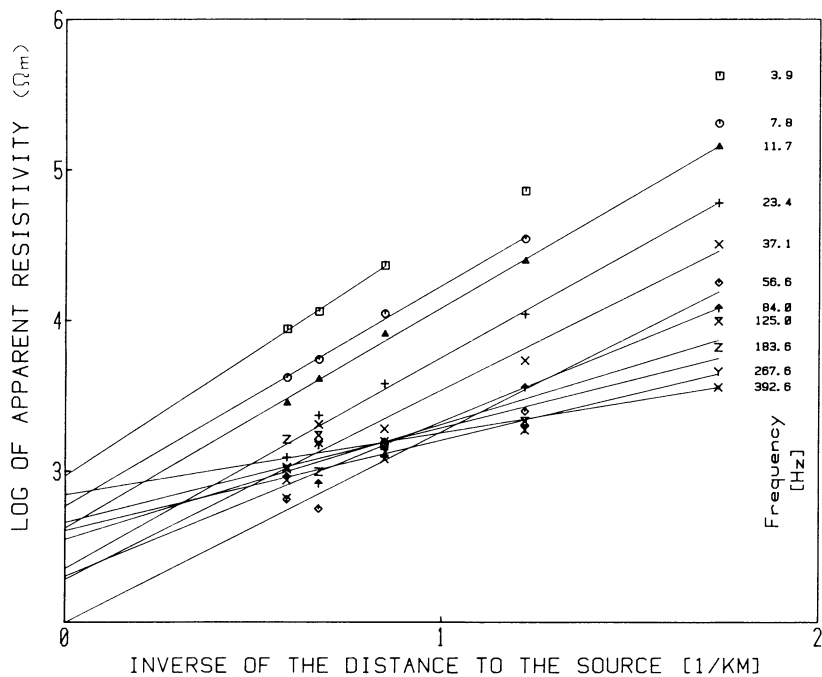


Fig. 7. Pulsed AMT data at a resistive site with broadside injection

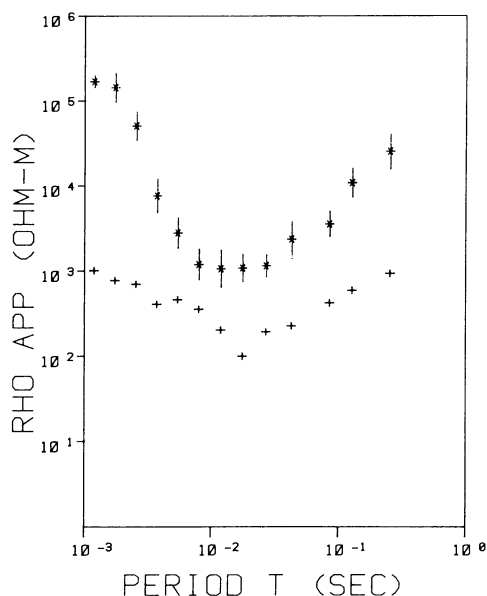


Fig. 8. Pulsed and natural AMT apparent resistivities at a resistive site. The $10^3 \Omega m$ overburden and substratum are typical of Jura limestones and the intermediate drop to $10^2 \Omega m$ probably arises from an intermediate layer of marls

when the location of the anomaly is already known approximately. With the receiving station placed in the vicinity of the anomaly, the source is moved to ever-increasing distances over horizontally layered terrain. In this situation both $\log \rho_a$ and ψ will retain a simple behaviour, easily extrapolated to the limit $1/r \rightarrow 0$ of very large distances.

Complex structures

With more complex structures our pulsed AMT method may become inadequate, especially if the source

itself is moved along a line traversed by geological accidents. Current flow will then assume patterns of distortions which are different for each injection site, rendering any attempt at extrapolation toward $1/r=0$ elusive. For structures which are not too distorted geologically, the method could retain some usefulness, however.

Comparison with other controlled source methods

The main characteristic of the method we have described is its closeness to classical AMT. This makes it possible to implement the pulsed technique with very few modifications and additions to a standard AMT system. By injecting current pulses the broadband feature is retained. Our band width is determined by the coils and the electronics we already had, to the period range $T=0.001-0.3$ s, but could probably have been extended by 1 decade on either side with the same pulse power. Because of power limitations it is not possible to inject the current at distances large enough to simulate an infinitely remote source. Our AMT receiving station is clearly in the near field of the source, but the distances are already large enough, with 1D structures at least, for extrapolations to infinite distances to be possible. In the methods described by Goldstein and Strangway (1975), Sandberg and Hohmann (1982) and Otten and Musmann (1982) all the power is injected in the form of harmonic variations. More power is thus available at a single frequency, and it then becomes possible to place the source at distances large enough to realize the far-field conditions. However, information is gathered only at one frequency at a time, even though the frequency can be varied, and it usually takes much longer to perform a single sounding. In these other methods it is necessary to inject large stationary currents; to achieve this goal with a minimum loss of power over the resistances of contact, elaborate

electrodes are required which must be inserted into specially prepared drill holes 2 or 3 m deep. This, again, is time-consuming labour. But if the far-field condition can be realized, these other methods can be implemented to study structures of any degree of complexity, although this may prove problematic since most complex structures generally comprise some highly resistive formations. These imply large penetration depths and, therefore, also large distances to realize the far-field condition. In this connection it is worth remembering that AMT is efficient in sounding complex structures only when they embody highly contrasted resistivities.

Conclusions

In principle AMT is a handy electromagnetic sounding tool for depths up to 1 or 2 km, but it is often plagued by two separate drawbacks: highly scattered data and apparent resistivities much larger than expected. These drawbacks have long been attributed to the sources which, instead of being the assumed distant tropospheric storms, are in fact more often man-made perturbations of local origin. We have indeed shown in Fig. 1 that in built-up areas the incident field has very poor spatial coherence. To improve the quality of AMT data we have looked into the possibility of utilizing artificially produced signals. Because of power limitations it was not possible to realize the ideal far-field condition, but by knowing the exact location of the source we were able to show that the data obtained can often be extrapolated to the far-field limit. The required condition is a sufficiently simple structure, as, for example, a horizontally stratified medium with a localized geological accident. In the course of this study we were able to show that apparent resistivities obtained from near-field sources are indeed systematically larger than far-field data, but the enhancement factor is strongly polarization dependent; in general it is appreciably larger for electrically collinear sources. These two observations therefore explain both the scatter and the increased resistivity typical of perturbed natural AMT. It also shows the importance of maintaining the same geometry between sounding site and injection station when implementing our new method.

The injection of current pulses gives our method the following desirable features:

- 1) The phenomenon is broadband; consequently, a standard natural AMT system can be used as receiving station.
- 2) The signal generator is simple to build and the entire system is only marginally more complex than a conventional AMT set-up.
- 3) No effort need be made to ensure the injection of a harmonic signal, simple metal spikes driven 20 cm into the ground are perfectly adequate.
- 4) Controlled source and natural source AMT results can be compared at once. With our method two controlled source soundings are still possible per work-day.

Appendix

The expressions for the field components given by Goldstein and Strangway (1975) refer to a horizontal two-

layer structure and can be expanded in the limit of large distances r . Taking the example of E_x and H_y , this yields:

$$E_x \cong \frac{1}{r^3} \left[A_1 + \frac{A_2}{r} + \dots + \frac{a_1 x^2}{r^2} + \frac{a_2 x^2}{r^3} + \dots + \frac{\alpha_1 y^2}{r^2} + \frac{\alpha_2 y^2}{r^3} + \dots \right], \quad (\text{A.1})$$

$$H_y \cong \frac{1}{r^3} \left[B_1 + \frac{B_2}{r} + \dots + \frac{b_1 x^2}{r^2} + \frac{b_2 x^2}{r^3} + \dots + \frac{\beta_1 y^2}{r^2} + \frac{\beta_2 y^2}{r^3} + \dots \right], \quad (\text{A.2})$$

where A_i, a_i, \dots, β_i are complex-valued constants. The terms with factors x^2/r^2 and y^2/r^2 describe the azimuthal dependence of the fields which could, therefore, also have been written more simply as

$$E_x \cong \frac{1}{r^3} \left[A_1(\theta) + \frac{A_2(\theta)}{r} + \dots \right], \quad (\text{A.3})$$

$$H_y \cong \frac{1}{r^3} \left[B_1(\theta) + \frac{B_2(\theta)}{r} + \dots \right], \quad (\text{A.4})$$

with $A_i(\theta)$ and $B_i(\theta)$ complex-valued functions of the azimuth θ . However, except for a constant factor the two functions $A_1(\theta)$ and $B_1(\theta)$ are identical, thus

$$\omega \mu_0 \rho_{xy} = \frac{|E_x|}{|H_y|} \cong \frac{|A_1(\theta) + A_2(\theta)/r|^2}{|B_1(\theta) + B_2(\theta)/r|^2} \cong \frac{|A_1^2[1 + 2A_2(\theta)/rA_1(\theta)]|}{|B_1^2[1 + 2B_2(\theta)/rB_1(\theta)]|}. \quad (\text{A.5})$$

Since $|A_2/rA_1|$ and $|B_2/rB_1| \ll 1$, this expression leads to

$$\ln \rho_{yx} \cong \ln \rho_a + \frac{f(\theta)}{r}, \quad (\text{A.6})$$

which clearly shows the linear behaviour of $\ln \rho$ vs $1/r$, provided the azimuth θ is kept constant. From Fig. 4 of Goldstein and Strangway (1975), as well as our own Fig. 3a and 4, it can be seen that $f(\theta)$ is much larger for a collinear than for a broadside geometry.

So far we have not looked at the theoretical behaviour predicted for the phase ψ as a function of the inverse distance $1/r$. The experimental data of Fig. 3b suggest that the phase can also be extrapolated linearly, but this linearity appears to break down at substantially smaller values of $1/r$ (i.e., at larger distances r). A simple linear extrapolation of the data of Fig. 3b is therefore not sufficient and we have carried out a best-fitting quadratic extrapolation over the four most distant sites. In other words, we have assumed that

$$\psi_{yx} = \psi + g_1(\theta)/r + g_2(\theta)/r^2, \quad (\text{A.7})$$

and derived the asymptotic phase ψ by extrapolating this expression to the limit $1/r=0$. The phase $\phi=45^\circ - \psi$ derived from this extrapolation can be compared with the natural AMT phase in Fig. 5. While we note a systematic difference between the two we have not, so

far, carried out as detailed a study of the phase as we have done in the present paper for the apparent resistivity. The behaviour of the phase is clearly more complicated and is less easily extrapolated to the far-field limit.

Acknowledgments. We gratefully acknowledge the help of Professor Weaver, as well as the financial support given by the Swiss National Science Foundation and the Geophysical Commission of the Academy of Natural Sciences.

References

- Fischer, G.: Magnetotelluric observational techniques on land. *Geophys. Surv.* **4**, 373–393, 1982
- Fischer, G., Le Quang, B.V.: Topography and minimization of the standard deviation in one-dimensional magnetotelluric modelling. *Geophys. J.R. Astron. Soc.* **67**, 279–292, 1981
- Fischer, G., Le Quang, B.V.: Parameter trade-off in one-dimensional magnetotelluric modelling. *J. Geophys.* **51**, 206–215, 1982
- Fischer, G., Schnegg, P.A.: The dispersion relations of the magnetotelluric response and their incidence on the inversion problem. *Geophys. J.R. Astron. Soc.* **62**, 661–673, 1980
- Gamble, T.D., Goubau, W.M., Clarke, J.: Magnetotellurics with a remote magnetic reference. *Geophysics* **44**, 53–68, 1979a

- Gamble, T.D., Goubau, W.M., Clarke, J.: Error analysis for remote reference magnetotellurics. *Geophysics* **44**, 959–968, 1979b
- Goldstein, M.A., Strangway, D.W.: Audio-frequency magnetotellurics with a grounded electric dipole source. *Geophysics* **40**, 669–683, 1975
- Otten, J., Musmann, G.: Aktive Audiomagnetotellurik bei Travale. *Protokoll Elektromagnetische Tiefenforschung, Neustadt a.W.*, pp. 183–188, 1982. See also Musmann, G., Otten, J.: Active audiomagnetotelluric application in geothermal areas. Abstract 13.18/IGA XVIII General Assembly, Hamburg, September 15–27, 1983 (p. 124)
- Sandberg, S.K., Hohmann, G.W.: Controlled-source audio-magnetotellurics in geothermal exploration. *Geophysics* **47**, 100–116, 1982
- Schnegg, P.-A., Le Quang, B.V., Fischer, G., Weaver, J.T.: Audio-magnetotelluric study of a structure with a reverse fault. *J. Geomagn. Geoelectr.*, in press 1984. See also Abstract 7.4 of Sixth Workshop on Electromagnetic Induction in the Earth and Moon, Victoria B.C., Canada, August 15–22, 1982
- Ward, S.H.: Controlled source electrical methods for deep exploration. *Geophys. Surv.* **6**, 137–152, 1983

Received December 20, 1983; Revised version March 19, 1984
Accepted March 21, 1984

Note added in proof

The linear behaviour of $\log \rho_{xy}$ (and similarly for $\log \rho_{yx}$) with the inverse distance r , as expressed by equation (A.6), has been observed experimentally to hold over a rather large range of $1/r$ values, as shown in Fig. 3a and 4. While this can be confirmed numerically it must be clearly stated that the linear range is in fact an *intermediate* range of distances. For very large separations, i.e. for very small values of $1/r$, the linear behaviour eventually breaks down. The leading terms are finally of order $1/r^2$ or even $1/r^4$. This, however, only applies to such large distances where the behaviour of $\log \rho_{xy}$ swings toward $\log \rho_a$ through a series of rapidly damped oscillations. These oscillations can be seen in some of the graphs of Goldstein and Strangway (1975) but are displayed much more clearly in the results of Otten and Musmann (1982). However, this oscillatory asymptotic behaviour corresponds to deviations from our linear extrapolations by amounts which are negligible in regard to the dispersion of the data. The phase behaves in similar fashion, but as we have observed (c.f. Fig. 3b) it may only exhibit a very small “intermediate” linear range, or none at all.

We are grateful to Dr. Weidelt for his help in clarifying this delicate point.